

Scientific paper

Some Factors Influencing Power and Energy Capabilities of RuO₂ Supercapacitors

Suzana Sopčić, Zoran Mandić* and Marijana Kraljić Roković

Faculty of Chemical Engineering and Technology, University of Zagreb, Marulićev trg 19, HR-10000 Zagreb, Croatia

* Corresponding author: E-mail: zmandic@fkit.hr

Received: 10-02-2014

Paper based on a presentation at the 4th RSE-SEE 2013 Symposium
on Electrochemistry in Ljubljana, Slovenia

Abstract

Ruthenium oxide electrodes prepared by different routes were studied and the results discussed in terms of the possibility of using these electrodes in high power/high energy supercapacitors. The supercapacitor electrodes were prepared by mixing RuO₂ particles with a binder (Nafion[®] or polyvinylidene fluoride) in various ratios. The results show that charging/discharging reaction of RuO₂ consists of at least two redox reactions taking place simultaneously at different rates. The contribution of each reaction in the overall process depends on the hydration of RuO₂ as well as on the type of binder and binder/RuO₂ ratio. From both energy and power capability of supercapacitors the best electrode composition would be hydrous RuO₂ with ~20% Nafion[®] as a binder. Asymmetric supercapacitors assembled with RuO₂ and activated carbon as a counter electrode gave 26 and 12 W h kg⁻¹ at average specific power of 5 W g⁻¹ for RuO₂/Nafion[®] and RuO₂/polyvinylidene fluoride, respectively.

Keywords: RuO₂; Supercapacitors; specific energy; Nafion[®]; PVDF

1. Introduction

Materials exhibiting pseudocapacitive behaviour are in the focus of research aiming to develop active, reversible and efficient electrodes for supercapacitor applications. Such materials must be able to store high charge and release it fast enough upon demand to ensure driving high power applications.¹ There are generally two classes of materials meeting such criteria: transition metal oxides and conducting polymers. Among them ruthenium oxide exhibits the most promising properties. It can be reversibly and reproducibly charged and discharged in a wide potential range and shows extraordinary chemical and morphological stability to undergo several thousands and in some cases even hundred thousands of charging/discharging cycles, without significant deterioration of its performance. When in amorphous and hydrous form, it can reach practical specific capacitance of up to 720 F/g² which is one of the highest specific capacitances ever observed in real applications.

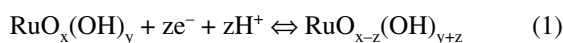
In spite of these outstanding properties, ruthenium oxide supercapacitors have still not achieved widespread commercial applications. The main obstacle is its high price and as a consequence, the ruthenium oxides supercapacitors

can nowadays be found only in some niche applications where the reliability and performance are more important than costs. In order to overcome these problems, many research efforts were made to design the electrodes with maximal utilization of ruthenium oxide and to increase charge content as much as possible. One direction of the improvement is the optimization of electronic conductivity and proton availability of the bulk ruthenium oxide since both quantities are necessary for its good performance.^{3–10} It is usually done by controlling the hydration of the ruthenium oxide particles annealing them at the temperatures around 150 °C where the good electron conductivity is achieved by removing the physically bound water present in the material and at the same time, preserving microcrystalline water enough to enable sufficiently fast proton diffusion.

Other directions of the increase of ruthenium oxide utilization were attempted by different preparation methods such as electrochemical deposition,^{6,11–13} oxidative chemical synthesis,⁵ sol-gel process,^{2,14–18} electrostatic spray deposition,^{7,19} electrophoretic deposition⁸ and hydrothermal synthesis.²⁰ Further improvement was made by the preparation of various composite materials usually with different forms of carbon.^{3,14,15,21–25} Such com-

posites effectively combined double layer capacitance of carbon with RuO₂ pseudocapacitance and at low RuO₂ loadings the capacitances as high as 1500 F/g,^{3,4,10} the values close to the theoretical capacitances of RuO₂, were achieved. In real applications, however, where substantial energy content is to be ensured, such low RuO₂ loadings are not practical and the bulk RuO₂, either in the form of thin film or as micro- to nano-sized particle assembly, must be used.

It is generally accepted that the electrochemical reaction accompanying the charging/discharging process involves simultaneous proton and electron exchange:



However, a lot of experimental evidences accumulated over the years demonstrated that the charging/discharging reaction of RuO₂ is more complex than it could be described by equation (1) and discerned from its cyclic voltammograms. This was explained by at least two different electrochemical reactions taking place simultaneously at different rates during charging/discharging process. Taking into account the reaction (1) it was proposed that the fast reaction was associated with the charging of outer surface area, whereas the slow process was due to the charging of deeper and less accessible oxide layers.^{26,27} Recent investigation by simultaneous cyclic voltammetry and QCM gravimetry^{1,10,28} showed that second reaction taking place in parallel to reaction (1) could be conveniently described by equation (2):



In contrast to the first mechanism which rate is limited by the diffusion of both electrons and protons in the hydrous oxide network, second reaction has more defined stoichiometry and proceeds through the incorporation of oxygen from water into the Ru(III) oxide during oxidation reaction and vice versa during reduction. Depending on whether water molecules stem from the solution side or from inside of hydrous layer, the process might be diffusionally or kinetically controlled. The RuO₂ charging/discharging mechanism of the reaction (2) type was recently termed dissociative adsorption of water.²⁹

In this work we focused on the preparation of RuO₂ electrodes with the intention to investigate the factors influencing relative rates of the two charging/discharging reactions and how their relative contributions affects supercapacitor performance from the high power/high energy standpoints. In order to be as close as possible to the practical applications for the preparation of the electrodes two binders, Nafion[®] and poly(vinylidene fluoride) (PVDF), were used. These binders have already shown significant impact on the electrochemical reaction of RuO₂.³⁰

2. Experimental

2.1. Chemicals and Materials

RuO₂ in hydrated and amorphous form, Nafion[®] 117 (5% solution in isopropyl alcohol) and poly(vinylidene fluoride) (PVDF) were purchased from Aldrich Chemie, N-methyl pyrrolidone (NMP) from Merck, isopropyl alcohol from T.T.T. (Croatia) and H₂SO₄ from Fluka. All solutions were prepared from bi-distilled water. X-ray diffraction and thermogravimetric analysis of the RuO₂ sample were published elsewhere.¹⁰

2.2. Preparation of the Electrodes

The electrodes for EQCM measurements were prepared by attaching the RuO₂ particles by cotton swab containing the material, and by using the drop of distilled water to fix the particles. In that way the particles were glued to electrode and randomly distributed assembly of particles on gold (A = 1.22 cm²) with more or less uniform distribution, was obtained.^{31,32} The RuO₂ used in these measurements was either thermally untreated or it was annealed at various temperatures from 70 to 200 °C. The amount of RuO₂ was determined by the resonant frequency changes caused by deposition of RuO₂ in dry state. The deposited mass of RuO₂ used in these studies was between 6–20 µg.

RuO₂/binder electrodes were prepared by casting of homogenized dispersions of RuO₂ particles in the solutions of appropriate binder on the glassy carbon electrode (A = 0.07 cm²). Two binders were used: Nafion[®] in isopropyl alcohol and PVDF in N-methyl pyrrolidone (NMP). The electrodes were dried for 24 hours at room temperature in the open air, in the case of Nafion[®], and in the vacuum at the temperature of 40 °C, in the case of PVDF. The masses of RuO₂ used for preparation of such composites were in the range of 0.04 to 0.46 mg whereas masses of binder were in the range of 0.025 to 0.4 mg, resulting in binder/RuO₂ ratio ranging between 0.25 and 4.

2.3. Assembling of Asymmetric Capacitor

The glassy carbon electrode was used as a substrate for both positive and negative electrodes. The positive electrode was electrode with RuO₂/Nafion[®] or RuO₂/PVDF composite, while the negative electrode was activated carbon mixed with PVDF binder. Electrodes were separated with cellulose membrane soaked in 0.5 mol dm⁻³ H₂SO₄ electrolyte.

2.4. Simultaneous Cyclic Voltammetry (CV) and Electrochemical Quartz Crystal Microbalance (EQCM) Measurements

Simultaneous cyclic voltammetry and EQCM measurements were carried out using Quartz Crystal Microbalance Digital Controller QCM200 (SRS, USA) connected to EG&G M263A potentiostat. The three-electrode sys-

tem was used with the working gold coated quartz crystal electrode made of 5 MHz AT-cut crystals of one inch diameter (Stanford Research Systems, SRS, USA). Each side of crystals was coated with titanium underlayer and gold. The surface area of electrode side which is in contact to an electrolyte was 1.22 cm² and inner surface area, so called piezoelectric area was 0.427 cm². The reference electrode was Ag/AgCl (3M KCl) while the counter electrode was Pt-foil. All measurements were performed in 0.5 M sulphuric acid in the potential range from -0.1 V to 1 V with scan rates of 0.05 and 0.2 V s⁻¹. Due to the good reproducibility of cyclic voltammograms only one cycle was taken for each measurement.

2. 5. Electrochemical Impedance Spectroscopy

Electrochemical impedance spectroscopy measurements were performed in the same three-electrode system with lock-in amplifier PAR 5210 which was connected to M263 potentiostat. The frequency range from 100 kHz to 10 mHz was scanned at the dc potential of 0.45 V vs. Ag/AgCl, with the amplitude of 5 mV.

3. Results and Discussion

3. 1. Cyclic Voltammetry and EQCM Investigations

Investigations of the pseudocapacitive reaction of RuO₂ was undertaken by cyclic voltammetry and simultaneous monitoring of mass change by EQCM on the hydrous samples as well as on samples annealed at various temperatures in the range from 70 to 200 °C. Fig. 1 shows the comparison of the results of the two samples, thermally untreated (Fig. 1a) and one treated at 130 °C (Fig. 1b). The cyclic voltammograms look similar showing almost rectangular

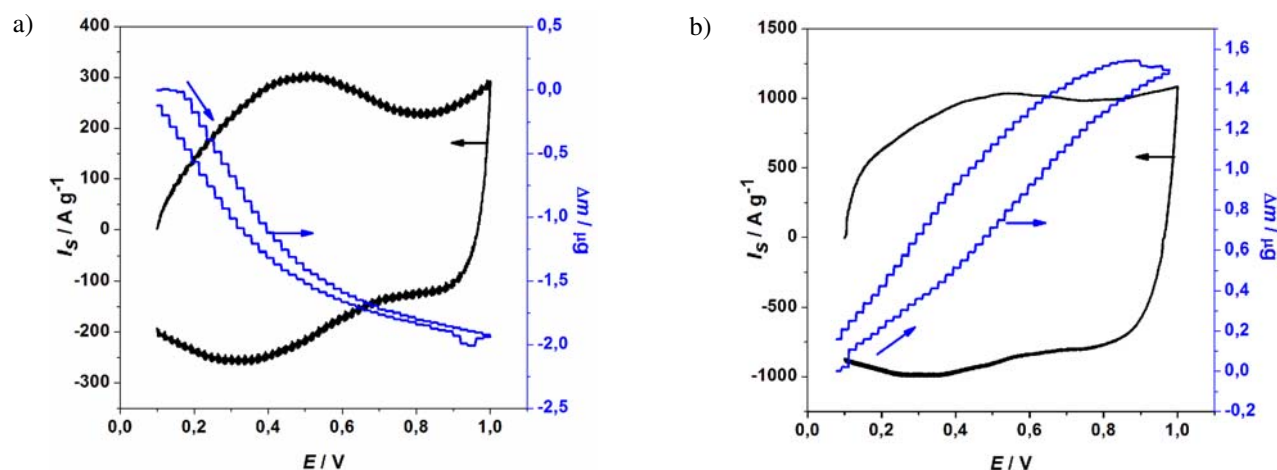


Figure 1. Simultaneous cyclic voltammograms and mass changes for the (a) hydrous, thermally untreated RuO₂ and (b) RuO₂ annealed at T = 130 °C. Scan rate: 0.2 V s⁻¹. Electrolyte: 0.5 M H₂SO₄.

shape and reversible electrochemical behaviour as would be expected for material having a potential to be used in supercapacitors. A broad anodic peak at about 0.5 V and its cathodic counterpart are dominant part of the cyclic voltammograms for the thermally untreated RuO₂. The peaks appear in the acidic media only and can be assigned to the reversible redox process accompanied by the sorption of protons and associated water molecules.^{33,34} Uneven current distribution throughout the investigated potential range points out the potential dependent capacitance of RuO₂. Low currents at more negative potentials of the cyclic voltammograms are explained by increased resistances caused by the bound water between oxide particles.^{3,4}

Thermal treatment of RuO₂ particles before the measurements has the profound effect on their electrochemical performance. Heating the samples removes almost all physically bound water resulting in the flattened cyclic voltammograms with more uniform current profiles. Overall charge increases with the annealing temperature

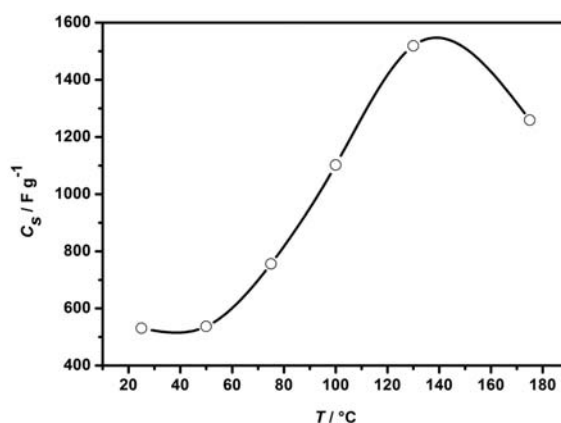


Figure 2. Dependence of specific capacitance of RuO₂ on the temperature pre-treatment. Specific capacitances were calculated by the integration of the cyclic voltammograms recorded at 0.05 V.

and the maximum charge can be extracted from the samples annealed at the temperatures around 130 °C (Fig. 2).

Another striking effect of the temperature pre-treatment is the change of the charging/discharging mechanism. Fig. 1 also shows simultaneous mass changes during the course of electrochemical oxidation and reduction of the two samples. Oxidation of the thermally untreated sample is accompanied by almost linear mass decrease while during reduction mass increase is observed. However, the sample annealed at 130 °C shows opposite behaviour, mass increase during oxidation and mass decrease during reduction. These results clearly indicate that electrochemical reaction of RuO₂ is a complex process consisting of at least two simultaneous reactions. As confirmed in the previous papers^{10,28} the two processes could be conveniently described by reactions (1) and (2). A dominant feature of the reaction mechanism described by equation (1) is a simultaneous proton and electron ingress during reduction and their expulsion during oxidation reaction. Since the reaction (1) involves the diffusion of protons and electrons which could limit the discharge rate of the oxide, high electronic and ionic conductivities are of the crucial importance in the design of high power supercapacitors based on RuO₂. On the other hand, reaction (2) proceeds with the oxygen atom incorporation in the oxide matrix during oxidation which is manifested as the overall mass increase of the electrode.

Both reactions occur simultaneously during charging and discharging of RuO₂. However, their relative rates and their contributions to the overall charge vary according to the sample treatment and experimental conditions. In highly hydrated and thermally untreated samples the reaction (1) is a dominant reaction in the overall process. In order to maximally utilize the material and to achieve capacitance and consequently specific energy as high as possible, the water content should be optimized. Removing the physically bound water enables less resistive electron pathways extending the depth of reaction layer and improving both available energy and power at the same time. However, decreasing the water content is less favourable for the proton diffusion. Consequently the contribution of the reaction (1) starts to decline and at pre-treatment temperatures above 130 °C the performance of charging/discharging process is determined in a great extent by reaction (2). By increase of temperature, the overall capacitance and energy start to decrease but on the other hand, since the diffusion as a slow process is eliminated, it should have favourable influence on the available power. The evidence for power improvement is more reversible cyclic voltammogram (Fig. 1b) obtained by temperature pre-treatment of RuO₂.

3. 2. Preparation and Properties of RuO₂ Electrodes

To confirm the conclusions made from simultaneous cyclic voltammetry and EQCM measurements in the previous section, bulk RuO₂ electrodes were prepa-

red and tested in the sulphuric acid electrolyte. The electrodes were prepared by mixing certain quantities of RuO₂ particles with a binder in order to keep mechanical integrity of the electrodes and to be as close to the practical applications as possible. Two binders, PVDF and Nafion[®], possessing different physico chemical properties were used since they were already shown to exert a considerable effect on the overall performance of RuO₂ electrodes.³⁰ The comparison of the cyclic voltammograms of RuO₂ electrodes prepared with Nafion[®] and PVDF as binders is given in Figure 3. Due to different influence of binder on RuO₂ particles, somehow higher specific current and slight peak separation was obtained in RuO₂ electrode with Nafion[®] as binder. The cyclic voltammograms exhibit similar features to those recorded at the EQCM electrodes. The values of specific currents achieved at EQCM measurement setup are much higher due to thinner layer and better electric contact between of RuO₂ particles with substrate as well as better contact of RuO₂ particles with electrolyte.

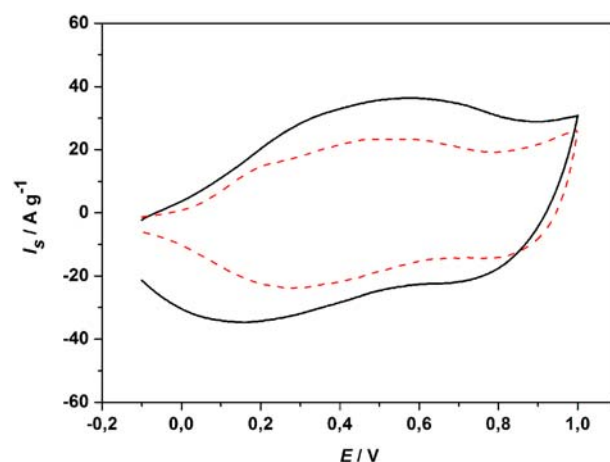


Figure 3. Cyclic voltammograms RuO₂/Nafion[®] (full line) and RuO₂/PVDF (dash line) electrodes with binder/RuO₂ ratio of 0.25, m(RuO₂) = 0.1 mg), examined in 0.5 M H₂SO₄ electrolyte. Scan rate: 0.05 V s⁻¹.

Although two cyclic voltammograms look similar, the complexity of the charging/discharging reaction of RuO₂ was revealed by dependence of specific capacitances of RuO₂ electrodes on the type and the quantity of the binder used and by the impedance spectroscopy measurements. Figure 4 shows the dependence of specific capacitances, C_s, of RuO₂ electrode on its composition. While specific capacitance in the presence of PVDF increases steadily with its mass increase, specific capacitances of RuO₂ electrodes in the presence of Nafion[®] follow more complex relationship. They increase with mass of Nafion[®] up to binder/RuO₂ ratio of approx. 0.25 and at higher ratios, specific capacitances start to decline.

Bode plots for two different compositions of RuO₂/Nafion[®] and RuO₂/PVDF electrodes are shown in Figs. 5a and 5b, respectively. As expected for the electrodes with good capacitive performance, the Bode plots of all samples consist of resistive behaviour at high and capacitive response at low frequencies. Depending on the sample composition and temperature pre-treatment, diffusion-like behaviour is observed in some cases in the middle frequency range. Diffusion-like behaviour is manifested in close to 45° phase angle and the slope of $\log Z - \log \omega$ of -0.5 in the middle frequency region. Such impedance responses were usually observed for the porous electrodes involving RuO₂ pseudocapacitive behaviour.^{6,35,36}

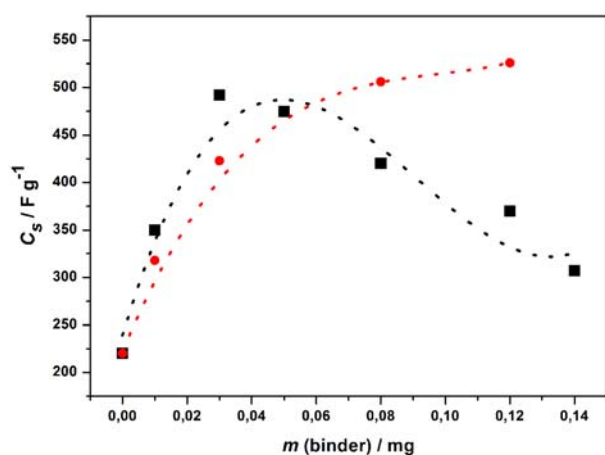


Figure 4. Characteristic dependence of the specific capacitance, C_s , on the mass of binder (squares – Nafion[®], circles – PVDF) in the composite electrodes with $m(\text{RuO}_2) = 0.1$ mg. Specific capacitances were calculated by the integration of the cyclic voltammograms recorded at 0.05 V.

Diffusion characteristics can be discerned in all impedance plots of RuO₂/PVDF electrodes and for RuO₂/Nafion[®] electrodes but only with low Nafion[®] content. Observed diffusion processes are frequently explained by the rate-limiting transport of ions, mainly protons, into the deeper layers of porous and hydrous RuO₂. By increasing the amount of Nafion[®] content diffusion process disappears from the middle frequency ranges. Taking into account higher capacitance obtained with RuO₂/Nafion[®] electrodes compared to RuO₂/PVDF electrodes (Fig. 3), it is evident that the presence of Nafion[®] facilitates the diffusion. In terms of two different electrochemical reactions represented by equations (1) and (2) it seems that Nafion[®] facilitates the contribution of reaction (1) in the overall capacitance of RuO₂ electrodes. Such composite electrode could be favourable for preparation of high power supercapacitors.

Since specific capacitance of RuO₂/Nafion[®] electrodes increases with Nafion[®] content (Fig. 4), as long as its mass does not exceed the critical value, it can be concluded that Nafion[®] has a positive impact on the RuO₂ overall performance.³⁶ The positive influence of Nafion[®] is demonstrated on energy but also on the power content, depending on its amount in overall mass of composite electrode. Obtained results indicate the ability of composite materials to give high specific energy with smaller Nafion[®] content or high specific power with higher amount of Nafion[®]. Higher Nafion[®] loadings are not so effective for energy probably due to increased ohmic resistances among RuO₂ particles and decreased utilization of RuO₂.

Difference of the impedance behaviour between the electrodes prepared with Nafion[®] and PVDF can be explained by different physico-chemical properties of these two macromolecules.³⁰ With its sulphonic groups attached

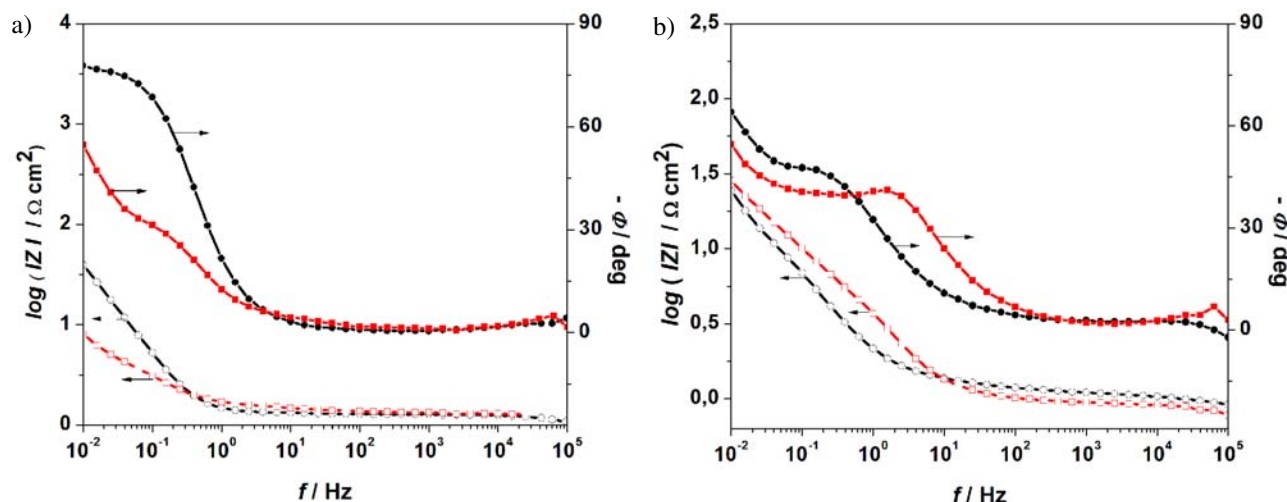


Figure 5. Bode plots of (a) RuO₂/Nafion[®] electrodes with binder/RuO₂ ratio of 4, $m(\text{RuO}_2) = 0.1$ mg (black curve) and 0.86, $m(\text{RuO}_2) = 0.46$ mg (red curve); (b) RuO₂/PVDF electrodes with binder/RuO₂ ratio of 0.25, $m(\text{RuO}_2) = 0.1$ mg (black curve) and 0.1, $m(\text{RuO}_2) = 0.04$ mg (red curve).

on the polymer backbone, Nafion[®] is attracted toward hydrous surface of RuO₂ effectively enveloping the particles interfering with the exchange of ions during charging and discharging process.

On the other hand, PVDF as a binder due to its hydrophobicity tends to form separate clusters within RuO₂ electrode leaving the surface of RuO₂ particles exposed to the solution. As a consequence, the pseudocapacitance reactions are not affected and reaction (1), contributes to the overall charge of the electrode displaying diffusional process in the impedance spectra (Fig. 5b).

As explained in the previous section, temperature pre-treatment of RuO₂ particles prior assembling the electrodes removes water from the hydrous layers of oxide and hinders proton diffusion decreasing the importance of the reaction (1) in the overall capacitance and leaving reaction (2) as the dominant reaction in the charging/discharging reaction. This behaviour is clearly visible in the impedance spectra of the RuO₂/PVDF electrodes where the process in the middle frequency range which is assigned to diffusion disappears (Figure 6).

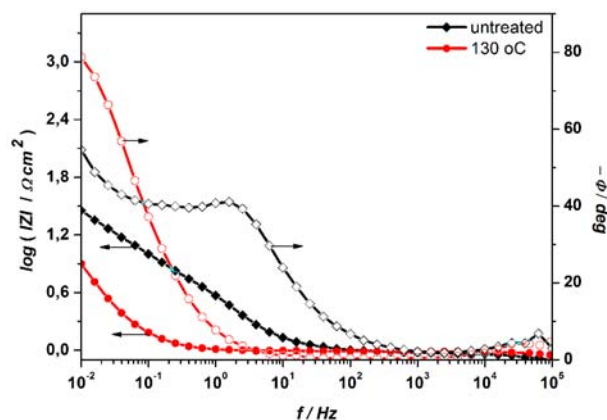


Figure 6. Bode plots of the thermally untreated RuO₂/PVDF sample (black curve) and one treated at 130 °C (red curve); binder/RuO₂ ratio = 0.1.

These results are in accordance with the results obtained by the simultaneous CV and EQCM measurements and they unambiguously demonstrate the existence of at least two types of charge in the pseudocapacitive reaction of RuO₂. Although total reaction mechanism is probably even more complex and composed of several simultaneous reactions including double layer charging,³³ two reactions described by equations (1) and (2) can reasonably explain the behaviour of RuO₂ electrodes. In order to achieve high energy RuO₂ supercapacitor it would be of a key importance to enable both reactions, taking place at the surface and in the deeper layer of oxide, to proceed at sufficiently high rates. In the case when Nafion[®]/RuO₂ ratio does not exceed the value

of 0.25, Nafion[®] promotes proton conducting pathways enhancing significantly charging/discharging capacitance. Nafion[®]/RuO₂ ratio of 0.25 consists 20% of Nafion[®] in the overall mass of the electrode and it would be the composition of choice for achieving excellent supercapacitor performance. If higher energy is required only, then RuO₂/PVDF electrode and RuO₂/Nafion[®] with smaller loading of Nafion[®] would be optimal compositions. However, if only high power is required then RuO₂/Nafion[®] with higher amounts of binder would be advisable.

3. 3. Performance of the Assembled RuO₂ Supercapacitors

RuO₂ electrodes were tested in the two-electrode configuration of the asymmetric supercapacitor with the counter electrode consisting of activated carbon. The quantities of activated carbon were carefully selected to match the energies of the two electrodes. Activated carbon was loaded on the glassy carbon support with PVDF as a binder and it was used for the negative electrode in the capacitor. Positive electrode was RuO₂/Nafion[®] or RuO₂/PVDF with binder/RuO₂ ratio of 0.25 and 0.5, respectively. In all cases the cell was charged up to 1 V while the current used for charging and discharging of such capacitors was 2 mA. Figure 7 shows the comparison of the performances of the supercapacitors based on RuO₂ electrodes made with Nafion[®] and PVDF as binders.

Cyclic voltammograms and constant current charging/discharging profiles of investigated supercapacitors are shown in Figs. 7a and 7b. Cyclic voltammograms are rectangular and, as expected, the higher specific current was obtained for RuO₂/Nafion[®] in comparison to RuO₂/PVDF capacitor (Fig. 7a). Specific energies of 26 and 12 W h kg⁻¹ were obtained for Nafion[®] and PVDF based RuO₂ electrodes, respectively, at average specific power of 5 W g⁻¹. During 1000 charging/discharging cycles the specific energy practically did not change for RuO₂/Nafion[®] capacitor while it slightly increased in the case of RuO₂/PVDF capacitor (Fig. 7c). Such increase can be explained by the progressive hydration enabling enhanced diffusion of protons at the both electrodes.

4. Conclusions

Charging/ discharging of RuO₂ is a complex process consisting of at least two reactions taking place simultaneously. Relative contributions of these two reactions depend on the hydrous state of RuO₂ and exact electrode composition. It has been found that the presence of Nafion[®] has favourable influence on the performance of RuO₂ electrodes but only up to 20% of overall content.

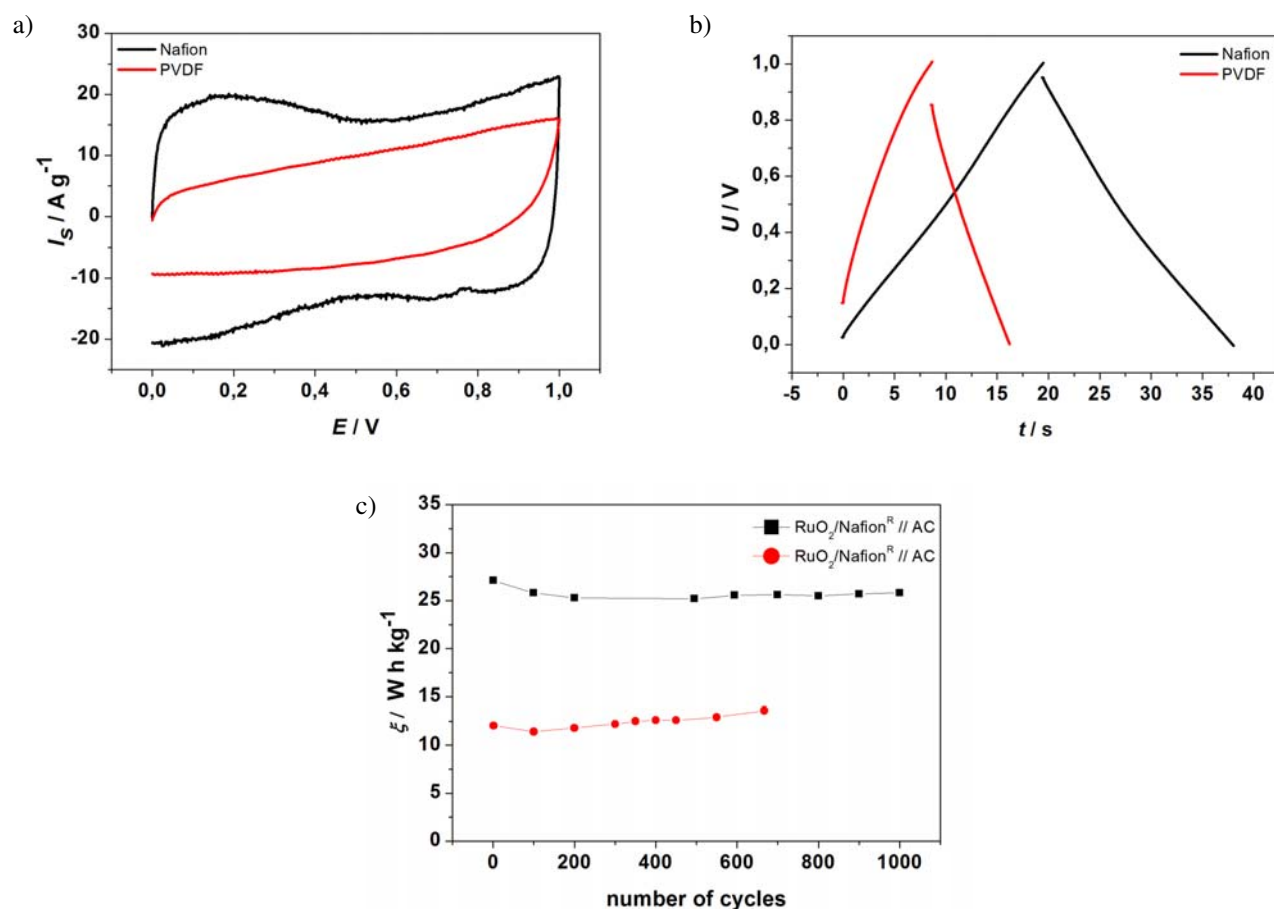


Figure 7. Electrochemical characterization of asymmetric RuO_2/AC capacitors. (a) Cyclic voltammograms of supercapacitors based on $\text{RuO}_2/\text{Nafion}^{\text{®}}$ (binder/ RuO_2 ratio = 0.25) and RuO_2/PVDF (binder/ RuO_2 ratio = 0.5) electrodes, $m(\text{RuO}_2) = 0.1 \text{ mg}$; (b) galvanostatic charge/discharge curves for the two assembled capacitors, (c) dependence of the specific energies during 1000 charge/discharge cycles.

Higher loadings are less effective. The $\text{RuO}_2/\text{Nafion}^{\text{®}}$ electrodes with 20% content are found to have the optimal composition for both high power and high energy supercapacitors. For higher energy RuO_2/PVDF compositions and for higher power $\text{RuO}_2/\text{Nafion}^{\text{®}}$ with higher $\text{Nafion}^{\text{®}}$ loadings are preferred.

5. Acknowledgements

The financial support for the Ministry of Science, Education and Sport (project 125-1252973-2576) is greatly appreciated.

6. References

1. B. E. Conway, *Electrochemical Supercapacitors*, Kluwer Academic/Plenum Publishers, New York, **1999**.
2. J. P. Zheng, P. J. Cygan, T. R. Jow, *J. Electrochem. Soc.*, **1995**, *142*, 2699–2703.
3. C. C. Hu, W. C. Chen, K. H. Chang, *J. Electrochem. Soc.*, **2004**, *151*, A281–A290.
4. O. Barbieri, M. Hahn, A. Foelske, R. Kötz, *J. Electrochem. Soc.*, **2006**, *153*, A2049–A2054.
5. K. H. Chang, C. C. Hu, *J. Electrochem. Soc.*, **2004**, *151*, A958A964.
6. C. C. Hu, Y. H. Huang, K. H. Chang, *J. Power Sources*, **2002**, *108*, 117127.
7. I. H. Kim, K. B. Kim, *J. Electrochem. Soc.*, **2006**, *153*, A383–A389.
8. J. H. Jang, A. Kato, K. Machida, K. Naoi, *J. Electrochem. Soc.*, **2006**, *153*, A321–A328.
9. A. Foelske, O. Barbieri, M. Hahn, R. Kötz, *Electrochem. Solid-State Lett.*, **2006**, *9*, A268–A272.
10. S. Sopčić, Z. Mandić, G. Inzelt, M. Kraljić Roković, E. Meštrović, *J. Power Sources*, **2011**, *196*, 4849–4858.
11. C. C. Hu, Y. H. Huang, *J. Electrochem. Soc.*, **1999**, *146*, 2465–2471.
12. K. Kvastek, V. Horvat-Radošević, *J. Electroanal. Chem.*, **2001**, *511*, 65–78.
13. V. Horvat Radošević, K. Kvastek, M. Vuković, D. Čukman,

- J. Electroanal. Chem.*, **2000**, *482*, 188–201.
14. J. Zhang, D. Jiang, B. Chen, J. Zhu, L. Jiang, H. Fang, *J. Electrochem. Soc.*, **2001**, *148*, A1362–A1367.
 15. V. Panić, T. Vidaković, S. Gojković, A. Dekanski, S. Milonjić, B. Nikolić, *Electrochim. Acta*, **2003**, *48*, 3805–3813.
 16. V. Panić, A. Dekanski, S. Gojković, V. Mišković-Stanković, B. Nikolić, *Mater. Sci. Forum*, **2004**, *453–454*, 133–138.
 17. V. Panić, A. Dekanski, S. Milonjić, R. Atanasoski, B. Nikolić, *Electrochim. Acta*, **2000**, *46*, 415–421.
 18. T. R. Jow, J. P. Zheng, *J. Electrochem. Soc.*, **1998**, *145*, 4952.
 19. I. H. Kim, K. B. Kim, *Electrochem. Solid State Lett.*, **2001**, *4*, A62–A64.
 20. K. H. Chang, C. C. Hu, *Electrochem. Solid-state Lett.*, **2004**, *7*, A466–A469.
 21. I. H. Kim, J. H. Kim, Y. H. Lee, K. B. Kim, *J. Electrochem. Soc.*, **2005**, *152*, A2170–A2178.
 22. M. Min, K. Machida, J. H. Jang, K. Naoi, *J. Electrochem. Soc.*, **2006**, *153*, A334–A338.
 23. M. Ramani, B. Haran, R. White, B. Popov, *J. Electrochem. Soc.*, **2001**, *148*, A374–A380.
 24. V. V. Panić, A. B. Dekanski, R. M. Stevanović, *J. Power Sources*, **2010**, *195*, 3969–3976.
 25. V. Panić, A. Dekanski, S. Gojković, S. Milonjić, V. Mišković-Stanković, B. Nikolić, *Mater. Sci. Forum*, **2005**, *494*, 235–240.
 26. S. Ardizzone, G. Fregonara, S. Trasatti, *Electrochim. Acta*, **1990**, *35*, 263–267.
 27. J. Risphon, S. Gottesfeld, *J. Electrochem. Soc.*, **1984**, *13*, 1960–1968.
 28. S. Sopčić, M. Kraljić Roković, Z. Mandić, A. Roka, G. Inzelt, *Electrochim. Acta*, **2011**, *56*, 3543–3548.
 29. P. Kurzweil, *J. Power Sources*, **2009**, *190*, 189–200.
 30. S. Sopčić, M. Kraljić Roković, Z. Mandić, *J. Electrochem. Sci. Eng.*, **2012**, *2*, 41–52.
 31. G. Inzelt, Z. Puskas, K. Nemeth, I. Varga, *J. Solid State Electrochem.*, **2005**, *9*, 823–835.
 32. S. Sopčić, M. Kraljić Roković, Z. Mandić, G. Inzelt, *J. Solid State Electrochem.*, **2010**, *14*, 2021–2026.
 33. W. Sugimoto, T. Kizaki, K. Yokoshima, Y. Murakami, Y. Takasu, *Electrochim. Acta*, **2004**, *49*, 313–320.
 34. S. Trasatti, G. Buzzanca, *J. Electroanal. Chem.*, **1971**, *29*, A1A5.
 35. R. Kötzt, M. Carlen, *Electrochim. Acta*, **2000**, *45*, 2483–2498.
 36. X. Liu, P. G. Pickup, *J. Power Sources*, **2008**, *176*, 410–416.

Povzetek

Elektrode rutenijevega oksida smo pripravili na različne načine. Dobljene rezultate smo diskutirali glede možnosti uporabe teh materialov v visokozmogljivih superkondenzatorjih. Superkondenzatorske elektrode smo pripravili z mešanjem RuO₂ delcev z veznim sredstvom (Nafion® ali polivinilidenfluorid) v različnih razmerjih. Rezultati kažejo, da je reakcija nabijanja in praznjenja sestavljena iz vsaj dve redoks reakciji, ki se odvijata istočasno z različno hitrostjo. Prispevek vsake izmed reakcij je odvisen od termične obdelave RuO₂ kot tudi vrste veznega sredstva in razmerja med veznim sredstvom in RuO₂. Na podlagi energije in delovne moči superkondenzatorja smo kot optimalno sestavo elektrode določili RuO₂, ki ni bil termično obdelan, z dodatkom ~20% Nafion® kot veznega sredstva. Pri povprečni specifični moči 5 W g⁻¹ proizvede asimetrični superkondenzator, ki je sestavljen in RuO₂ in aktiviranega ogljika kot številne elektrode, 26 in 12 W h kg⁻¹ za RuO₂/Nafion® oziroma RuO₂/polivinilidenfluorid.